Journal of Physics: Conference Series **2667** (2023) 012030 doi:10.1088/1742-6596/2667/1/012030

Interacting two-mode model for ultracold quantum interferometers

Cosetta Baroni

Institut für Quantenoptik und Quanteninformation (IQOQI), Österreichische Akademie der Wissenschaften, A-6020 Innsbruck, Austria

E-mail: cosetta.baroni@uibk.ac.at

Giacomo Gori

Institut für Theoretische Physik, Universität Heidelberg, D-69120 Heidelberg, Germany

E-mail: gori@thphys.uni-heidelberg.de

Maria Luisa Chiofalo

Dipartimento di Fisica "Enrico Fermi", Università di Pisa and INFN, Largo B. Pontecorvo 3, I-56127 Pisa, Italy

E-mail: marilu.chiofalo@unipi.it

Andrea Trombettoni

Department of Physics, University of Trieste, Strada Costiera 11, I-34151, Trieste, Italy

E-mail: atrombettoni@units.it

Abstract. Ultracold gases provide an excellent platform for the realization of quantum interferometers. In the case of implementations based on Bose-Einstein condensates in double well potentials, an effective two-mode model allows to study how the interactions among particles affect the sensitivity of the interferometer. In this work we review the properties of such a model and its application to interferometric protocols, focusing on the achievable sensitivity in the presence of interactions turned on. In particular we study the full interferometric sequence when the initial state is a Twin Fock state, which is perfectly number squeezed. We found that in the presence of interactions and for certain values of the holding time in which a phase difference between the two modes is accumulated, the same sensitivity as in the non interacting case is recovered when using the population imbalance between the two wells as observable. Finally, we characterize the behaviour of the sensitivity by looking at the δ-derivative and the variance of the operator used for the measurement and studying the squeezing parameters.

1. Introduction

The aim of quantum interferometry is in general to resolve the phase shift ϕ between two sources generated by the physical effect under investigation, taking advantage of quantum resources and improve upon the performance of classical interferometers [1, 2]. The precise modelization of the task depends on the particular physical system used to implement the quantum interferometer, but a first information can be obtained using simplified models to describe the sources entering the interferometric scheme, such as effective two-mode (2M) models in the case of atomic iterferometers based on a Bose-Einstein condensate in a double well. In this way one can study the effect of interactions among particles on the sensitivity of the interferometer. This is particularly important since from one side one can obtain an improvement of the sensitivity taking advantage of interactions in the splitting process or to generate squeezed input states, but from the other side the presence of interactions in specific steps of the interferometric scheme may lead to a degradation of the sensitivity [2]. The effects of the presence of interactions and the connection with entanglement have been intensively studied [3, 4, 5, 6, 7, 8, 9, 10, 11, 12], see as well the reviews [2, 13, 14].

In general interferometric schemes as implemented in quantum optics contexts, a splitting process between two sources, realised via a beam splitter, is needed in order to accumulate a phase shift [2]. After a phase shift is accumulated, recombination of the two sources is performed, thanks to a second beam splitter. This shows that a crucial role in any interferometric scheme is provided by the beam splitter. Interaction affects the beam splitter giving non-linear contributions to the scaling of the phase sensitivity [4, 15, 16, 17, 19, 20, 21], more references being in [13].

Ultracold gases provide an ideal platform to implement quantum interferometric tasks [2]. The rationale is that in these systems interactions can be tuned directly, using Feshbach resonances [22] or confining the system in lower dimensions [23, 24, 25], but also indirectly, modifying the ratio between the kinetic and the interaction terms [2]. This can be achieved in double- and multi- well potentials [26, 27, 28, 29] by varying the energy barrier between the wells, resulting in a tunable hopping coefficient J. In a double well, the effective dynamics is described by a 2M model [26], which can be then used to model interferometric scheme in double well potentials. The goal of this paper is to review the use and the properties of the 2M model used in ultracold quantum interferometers, and focus on the interferometers sensitivity when the interactions are turned on during all the different steps of the interferometric process.

The presentation is organized according to the following scheme. In Section 2 we introduce the 2M model. We remind in Section 3 basic properties of quantum interferometery used in the study of the performance of ultracold quantum interferometers. In Section 4 we provide the details of the interferometric protocol and discuss how to characterize the behaviour of the phase sensitivity. In Section 5, focusing on the Twin Fock state as initial state, we study the behaviour of the interferometer sensitivity varying the holding time, the particle number, and the interaction energy, commenting our results with known findings in literature. Our conclusions are presented in Section 6.

2. The model

In this section we introduce the model we are going to use in the rest of the paper, the 2M model, encoding the many-body description of N condensed bosons in a double well potential in a 2M Bose-Hubbard Hamiltonian with the two modes, $\hat{a}$ and $\hat{b}$, well separated in energy from the other ones [13, 26, 30, 31, 32]:

$$\hat{H} = -J(\hat{a}^\dagger\hat{b} + \hat{b}^\dagger\hat{a}) + \frac{U}{2}(\hat{a}^\dagger\hat{a}^\dagger\hat{a}\hat{a} + \hat{b}^\dagger\hat{b}^\dagger\hat{b}\hat{b}) + \frac{\delta}{2}(\hat{a}^\dagger\hat{a} - \hat{b}^\dagger\hat{b}) \; . \tag{1}$$

In (1) $\hat{a}^\dagger$ and $\hat{b}^\dagger$ create a particle in the left and right well, respectively. The parameters entering (1) are: J the tunnelling strength, U the particle interaction in each mode, and δ the energy shift between the two modes. Since during the interferometric process U, J and δ can be varied, they are time-dependent. Through this work we set $\hbar = 1$. The system is well described in the Fock space, the elements of which are denoted by $|n\rangle \equiv |n_a = n; n_b = N - n\rangle$. We additionally introduce the number operators $\hat{n}_a = \hat{a}^\dagger \hat{a}$ and $\hat{n}_b = \hat{b}^\dagger \hat{b}$, and the population imbalance between the two wells $z = \frac{n_a - n_b}{N}$.

Given a state $|\psi\rangle = \sum_{n=0}^{N} c_n(t)|n\rangle$, the dynamics of the system can be described by the time evolution of the coefficients $c_n(t) = \langle n|\psi(t)\rangle$ obtained by solving the Schrödinger equation $i\frac{\partial \psi(t)}{\partial t} = H\psi(t)$ with H given by (1).

By introducing the pseudo-spin operators $\hat{J}_x = \frac{1}{2}(\hat{a}^\dagger \hat{b} + \hat{b}^\dagger \hat{a})$, $\hat{J}_y = \frac{1}{2i}(\hat{a}^\dagger \hat{b} - \hat{b}^\dagger \hat{a})$ and $\hat{J}_z = \frac{1}{2}(\hat{a}^\dagger \hat{a} - \hat{b}^\dagger \hat{b})$, the Hamiltonian (1) can be written as $\hat{H} = -2J\hat{J}_x + \frac{U}{2}\hat{J}_z^2 + \delta \hat{J}_z$. In the Bloch sphere representation the tunnelling term rotates a state around the x-axis, while the interaction term twists its components above and below the equator respectively to the right and to the left and the twist rate increases increasing the distance from the equator, offering the possibility to create spin squeezed states [33].

3. Phase sensitivity of a quantum interferometer

Spin squeezed states can be used to perform interferometric tasks better than the shot noise limit $\Delta\phi = 1/\sqrt{N}$ and several criteria to determine if a state is squeezed have been introduced [34]. The parameter ξ_N is related to the variance of a spin component being smaller than the shot-noise limit $J/2$ for a coherent spin state so that the criterion reads $\xi_N^2 \equiv \frac{2}{J}(\Delta \hat{J}_{\perp,min})^2 < 1$. One can also defined the quantity $\xi_S^2 \equiv N\frac{(\Delta \hat{J}_{\perp,min})^2}{\langle \hat{J}\rangle^2}$, so that the criterion reads $\xi_S^2 < 1$. In order to measure the useful squeezing, the quantity $\xi_R \equiv \sqrt{2J}\frac{\Delta \hat{J}_{\perp,min}}{\langle \hat{J}\rangle}$ has been also introduced.

To estimate the phase ϕ accumulated after an interferometric sequence, one can measure an observable $\hat{O}$ having a ϕ-dependent expectation values and, from error propagation, it follows that

$$\Delta\phi = \frac{\Delta \hat{O}}{\left|\partial\langle \hat{O}\rangle/\partial\phi\right|} = \frac{\xi}{\sqrt{N}} , \tag{2}$$

where $\Delta \hat{O} = \sqrt{\langle \hat{O}^2\rangle - \langle \hat{O}\rangle^2}$ is the variance of the operator $\hat{O}$.

4. The interferometric protocol

In this section we introduce the complete interferometric sequence, consisting of a first beam splitter, acting for a time T_{BS}, a phase accumulation stage, during an holding time T_H, and a second beam splitter, acting again for a time T_{BS}. In the following all quantities are expressed in units of J.

The goal is to determine the sensitivity with which this interferometric sequence is able to measure the parameter δ. An example of the protocol used is the following: the first beam splitter is realized by allowing the particles to tunnel from one well to the other for an optimal time, to be determined, afterwards the tunnelling coupling is suddenly switched off. Notice indeed that the best splitting process is found for an abruptly turning off of the tunnelling coupling [4]. Asymmetry between the wells is introduced by setting $\delta \neq 0$. The system evolves with these conditions for an arbitrary holding time T_H, in which a phase $\phi = \int \delta dt$ is accumulated. After this process, the second beam splitter acts, by setting $\delta = 0$ and allowing the particles to tunnel again for the same time, T_{BS}, used for the first beam splitter.

If interactions are present, they affect the whole process described above. A parametric scan of the aforementioned protocol around the parameter δ can be performed in order to find the sensitivity at each holding time: once the behaviour of the operator used for the measurement has been obtained as a function of δ, the sensitivity is defined as

$$\Delta\delta \equiv \frac{\Delta\langle \hat{O}\rangle}{|\partial\langle \hat{O}\rangle/\partial\delta|}\bigg|_{min} . \tag{3}$$

Finally, the whole interferometric procedure is repeated for different holding times.

Notice that in the following discussion decoherence phenomena are not taken into account (atoms can be held up to $\sim$ 100ms to 10s, according to the cases, without significant decoherence effects [35]).

5. Initial state Twin Fock

The so-called Twin Fock state, $|\frac{N}{2}, \frac{N}{2}\rangle$, is a perfectly number squeezed state in the sense of the squeezing parameter ξ_N^2 and can allow for interferometry beyond the classical limit, improving the sensitivity near the Heisenberg limit [36]. If no energy shift is present between the wells, the particles are equally distributed among them and a population imbalance measurement would give no information about phase accumulation, so that other operators but z, such as $\hat{J}_z^2$ or the parity operator $\hat{\Pi}_b = e^{i\pi n_b}$ [37], have to be used in order to make a meaningful measurement. In the following we choose to investigate measurements performed using the parity operator as observable, which behaviour, as a function of δ, is described, in the non interacting case, by $P_{\frac{N}{2}}(\cos 2\phi)$, where $P_{\frac{N}{2}}$ are the Legendre polynomials of order $N/2$ and $\phi = \int \delta dt$.

5.1. *Results for $U = 0$ and $N = 2$*

In this paragraph we report the results of analytical calculations for the simplest case of $N = 2$ and without interactions.

We realized the beam splitters by letting the particles tunnelling for a time $T_{BS} = \frac{\pi}{4J}$ without asymmetries between the wells ($\delta = 0$), so that the system evolves according to the Hamiltonian $H = -J(a^\dagger b + b^\dagger a)$. During the phase accumulation stage the state evolves according to the Hamiltonian $H = \frac{\delta}{2}(n_a - n_b)$ for a time T_H. At the end of the full interferometric sequence, the coefficients $c_n(t)$, are given by

$$c_2(T_{BS}) = \frac{\sin(\delta T_H)}{\sqrt{2}}\ , c_1(T_{BS}) = -\cos(\delta T_H)\ , c_0(T_{BS}) = -\frac{\sin(\delta T_H)}{\sqrt{2}}\ . \tag{4}$$

The expectation value, the variance and the δ-derivative of the parity operator are then

$$\langle\hat{\Pi}\rangle = \sum_n \langle n|e^{i\pi\hat{n}_b}|n\rangle = -\cos(2\delta T_H)\ , \Delta\hat{\Pi} = \sin(2\delta T_H)\ , \frac{\partial\langle\hat{\Pi}\rangle}{\partial\delta} = 2T_H\sin(2\delta T_H)\ . \tag{5}$$

According to (3) the sensitivity is thus

$$\Delta\delta = \frac{1}{2T_H} \tag{6}$$

and it scales as $\frac{\alpha}{N^\beta T_H^\gamma}$, with $\alpha = \beta = \gamma = 1$ according to the Heisenberg limited sensitivity.

In the following we describe how the sensitivity is influenced by varying the holding time for different values of the interaction energy and the particle number.

5.2. *Non interacting case*

As predicted by the analytical results presented in the previous paragraph, in the non interacting case the sensitivity is near the Heisenberg limit, as shown in the following figures and tables. The state evolution during the interferometric process is represented on the Bloch sphere in Fig. 1, the blue circle representing the variance along the J_i axes, $\Delta\hat{J}_i$. If there are not interactions, the initial and final states are perfectly number squeezed states with vanishing mean spin length.

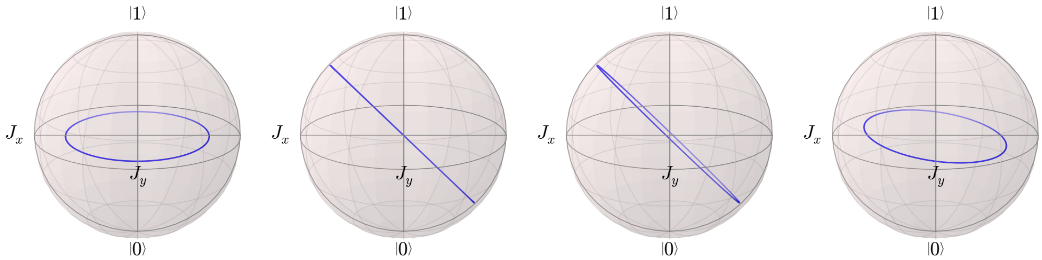

Figure 1. Variance along the J_i axes represented on the Bloch sphere in case of a Twin Fock as initial state. *First:* initial state; *Second:* after the first beam splitter; *Third:* after the accumulation stage; *Last:* after the full interferometric sequence. $U = 0$ and $N = 10$.

In Fig. 2 the sensitivity $\Delta\delta$ is plotted as a function of the holding time T_H for different values of the particle number N (left panel) and as a function of N for different values of T_H (right panel). In order to compare with the Heisenberg limited sensitivity, the behavior is fitted with the function $\Delta\delta = \frac{\alpha}{N^\beta T_H^\gamma}$ in the first case and with the function $\Delta\delta = \frac{\alpha}{N^\beta T_H}$ in the second case. The resulting coefficients are reported in Tables 1. We find that β remains constant and close to unity for different values of the particle number and holding times, in agreement with the Heisenberg limited sensitivity as expected from Eq. (6).

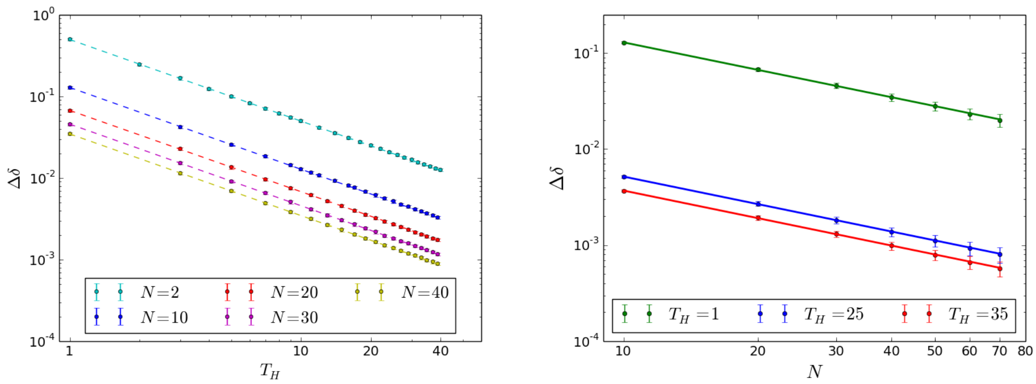

Figure 2. *Left:* Sensitivity $\Delta\delta$ as a function of the holding time T_H for different values of the particle number N. *Right:* Sensitivity $\Delta\delta$ as a function of the particle number N at different holding times T_H. Dashed lines are fitting curves, see text.

5.3. Varying interactions

In this paragraph we analyse the behaviour of the system for different values of the interaction energy U at fixed particle number $N = 10$.

The goal is to check whether some values of the holding time exist for which a good sensitivity, hopefully better than the one for the non interacting case, could be reached. The joint effect of interactions and asymmetry in the two wells leads to a measurable population imbalance z after the full interferometric sequence, so that z becomes a measurable observable, in opposition to what happens in the absence of interactions. In the following only repulsive interactions ($U > 0$) are considered.

N	α	γ	β
2	0.999 ± 0.002	0.999 ± 0.001	1.00 ± 0.02
10	1.28 ± 0.01	0.997 ± 0.004	1.00 ± 0.02
20	1.35 ± 0.03	1.007 ± 0.008	1.00 ± 0.03
30	1.37 ± 0.04	1.005 ± 0.006	1.00 ± 0.02
40	1.38 ± 0.03	1.005 ± 0.007	1.00 ± 0.03

T_H	α	β
1	1.37 ± 0.04	0.99 ± 0.04
25	1.37 ± 0.04	0.99 ± 0.04
35	1.37 ± 0.04	1.01 ± 0.02

Table 1. *Left:* Fit coefficients for $\Delta\delta$ *vs* T_H for different values of the particle number N obtained by fitting the data in the left panel of Fig. 2 with the function $\Delta\delta = \frac{\alpha}{N^\beta T_H^\gamma}$. *Right:* Fit coefficients for $\Delta\delta$ *vs* N for different values of the holding time T_H obtained by fitting the data in the right panel of Fig. 2 with the function $\Delta\delta = \frac{\alpha}{N^\beta T_H}$.

In Fig. 3 the sensitivity $\Delta\delta$ is plotted as a function of the holding time T_H at a fixed particle number $N = 10$, for different values of the interaction energy U using either the parity operator $\hat{\Pi}_b$ (left panel) or the population imbalance z (right panel) as observables. We can see that with the interactions always turned on there is no gain in sensitivity with respect to the non interacting case, neither using parity nor population imbalance measurements. A more complete study with time-dependent interactions would require the use of the Fisher information, as carried out in [7]. In the case of z measurements two kind of minima in the sensitivity are identified: primary

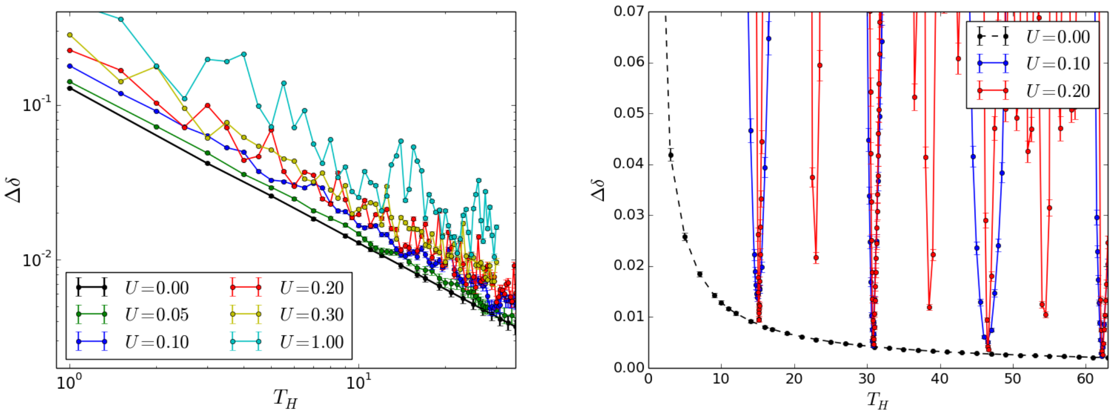

Figure 3. Sensitivity against holding time varying interaction energy at fixed $N = 10$, obtained from parity measurement (left) and population imbalance measurements (right); the dashed line, indicating the case $U = 0$, is obtained always from parity measurements.

ones, close to the non interacting results (dashed black line in the left panel), and secondary ones, occurring, respectively, at times T_H such that: $T_{H_{\rm I}} + T_{BS} = m\frac{\pi}{U}$, $T_{H_{\rm II}} + T_{BS} = (2m+1)\frac{\pi}{2U}$ where m is a integer. After the holding time the coefficients $c_n(t)$ have evolved according to $c_n(T_H) = e^{-i\left(\frac{U}{2}(2n(n-N)+N(N-1))+\frac{\delta}{2}(2n-N)\right)T_H} c_n(T_{BS})$. We see that $e^{-iU(T_{H_{\rm I}}+T_{BS})} = \pm 1$ for times corresponding to primary minima, and $e^{-iU(T_{H_{\rm II}}+T_{BS})} = \pm i$ for times corresponding to secondary minima. The period of the minima corresponding to the same class is π/U. The values of δ that give the best sensitivity are those for which the term $e^{-i\frac{\delta}{2}} \sim 1$ in $c_n(T_H)$. Even though the values of the sensitivity achieved for the primary minima are close to the ones obtained in the non interacting case, no gain is reached.

Additionally, we have checked the effect of varying the particle number N at fixed interaction energy values $U = 0$ and $U = 0.1$ on the achievable sensitivity $\Delta\delta$. We found that by increasing the particle number, the sensitivity worsen for finite interaction energy with respect to the non interacting case.

5.4. *Characterizing the behaviour of the sensitivity*

We now characterize the behaviour of the sensitivity by looking at the δ-derivative and the variance of the operator used for the measurement and studying the squeezing parameters ξ_N^2 and ξ_S^2, defined in Section 3.

As expressed in (3), the δ-derivative and the variance of the operator chosen to perform the measurement are important quantities in defining the sensitivity with which the interferometer can determine the energy difference δ between the two wells. In Fig 4 we present the results of our simulation for the sensitivity as a function of the holding time, together with the results obtained for the δ-derivative and the variance of the parity operator $\hat{\Pi}_b$ (left panel) and the population imbalance z (right panel) in the case of finite interaction energy $U = 0.1$ and $N = 10$ particles. In particular we notice that, when z is used to perform the measurement, the primary and secondary minima identified in the right panel of Fig. 3 coincide with precise values of the δ-derivative and the variance. In the right panel of Fig 4 we show that primary minima of $\Delta\delta$ correspond to points for which the δ-derivative of z has a local maximum and the variance of z has a minimum, while secondary minima correspond to maxima of the δ-derivative and local minima of the variance. Maxima of $\Delta\delta$ are associated to maxima of the δ-derivative and minima of the variance.

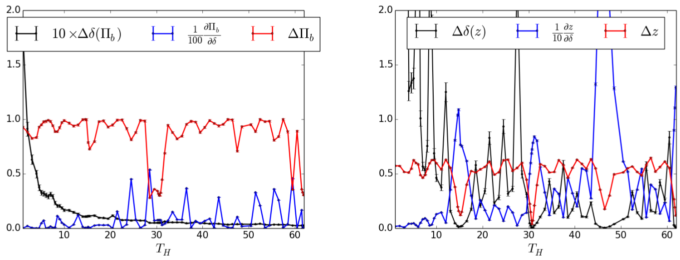

Figure 4. Sensitivity $\Delta\delta$, δ-derivative $\frac{\partial\langle\hat{O}\rangle}{\partial\delta}$, and variance $\Delta\hat{O}$ of the operator $\hat{O}$ as functions of the holding time at fixed $U = 0.1$ and $N = 10$. *Left:* $\hat{O} = \hat{\Pi}_b$. *Right:* $\hat{O} = z$. For better readability, when needed, different quantities have been rescaled.

In order to understand the structure of maxima and minima of $\Delta\delta$ as a function of the holding time when z measurements are used, we calculated the squeezing parameters ξ_N^2 and ξ_S^2 at the end of the interferometric sequence. Primary minima of $\Delta\delta$ are found at holding times for which the final states result squeezed according to both the considered parameters. Both ξ_N^2 and ξ_S^2 are found to be smaller than unity where the δ-derivative of J_z has a maximum (note that $J_z = \frac{Nz}{2}$). Secondary minima of $\Delta\delta$ are found when the final states result squeezed only in the sense of ξ_N^2. Finally, maxima of $\Delta\delta$ correspond to final states that are not squeezed at all.

6. Conclusions

Our results show the richness and the interest of studying and characterizing the performance of an ultracold quantum interferometer. Our interferometric sequence is very simple: it is made up of a first beam splitter, a phase accumulation stage, and a second beam splitter identical to the first. In the chosen interferometer scheme, with the interaction turned on, during the beam splitter process the energy offset δ does not act and the tunnelling constant J is simply set equal to zero. Dealing with the Twin Fock as initial state, we found that a value of the sensitivity close to the one for the non interacting case is found at specific phase accumulation times when population imbalance measurements are performed.

As future works, motivated by the results presented in this paper, we mention the interest in considering other initial states in optimized interferometric schemes and in studying the Loschmidt echo [38], and the possibility of systematically study the interplay between interactions always turned on and projective measurements performed during the phase accumulation stage.

Acknowledgments
G.G. and A.T. thank valuable discussions with participants of QTS12 - XII International Symposium on Quantum Theory and Symmetries in Prague (July 2023).

References

[1] Cronin A D, Schmiedmayer J and Pritchard D E 2009 *Rev. Mod. Phys.* **81** 1051
[2] Pezzé L, Smerzi A, Oberthaler M K, Schmied R and Treutlein P 2018 *Rev. Mod. Phys.* **90**, 035005
[3] Pezzé L and Smerzi A 2006 *Phys. Rev. A*, **73**, 011801
[4] Pezzé L, Smerzi A, Berman G P, Bishop A R and Collins L A 2006 *Phys. Rev. A*, **74**, 033610
[5] Burkov A A, Lukin M D and Demler E 2007*Phys. Rev. Lett.* **98** 200404
[6] Pezzé L and Smerzi A 2009 *Phys. Rev. Lett.* **102** 100401
[7] Grond J, Hohenester U, Schmiedmayer J and Smerzi A 2011 *Phys. Rev. A* **84** 023619
[8] Pawlowski K, Fadel M, Treutlein P, Castin Y and Sinatra A 2017 *Phys. Rev. A* **95** 063609
[9] Baroni C 2017 *Effects of Interactions on the Performance of Ultracold Quantum Interferometers* (Master's Thesis, University of Pisa, Pisa, Italy)
[10] Wrubel J P, Schwettmann A, Fahey D P, Glassman Z, Pechkis H K, Griffin P F, Barnett R, Tiesinga E and Lett P D 2018 *Phys. Rev. A* **98** 023620
[11] Zhang Q and Schwettmann A 2019 *Phys. Rev. A* **100** 063637
[12] Baroni C, Gori G, Chiofalo M L and Trombettoni A 2020*Condensed Matter* **5** 2
[13] Gross C 2012 *J. Physics B: At. Mol. Opt. Phys.* **45** 103001
[14] Braun D, Adesso G, Benatti F, Floreanini R, Marzolino U, Mitchell M W and Pirandola S 2018 *Rev. Mod. Phys.* **90** 035006
[15] Huang Y P and Moore M G 2008 *Phys. Rev. Lett.* **100** 250406
[16] Grond J, von Winckel G, Schmiedmayer J and Hohenester U 2009 *Phys. Rev. A* **80** 053625
[17] Jin G R, An Y, Yan T and Lu Z S 2010*Phys. Rev. A* **82** 063622
[18] Chwedeńczuk J, Hyllus P, Piazza F and Smerzi A 2012 *New J. Phys.* **14** 093001
[19] Mullin W J and Laloë F 2015 *Phys. Rev. A* **91** 053629
[20] Prakash H and Mishra D K 2016 *J. Opt. Soc. Am. B* **33** 1552
[21] Berrada T, van Frank S, Bücker R, T.Schumm T, Schaff J - F, Schmiedmayer J, Julía-Díaz B and Polls A 2016 *Phys. Rev. A* **93** 063620
[22] Bloch I, Dalibard J and Zwerger W 2008 *Rev. Mod. Phys.* **80** 885
[23] Castin Y 2004 *Journal de Physique IV Proceedings* **116** 89
[24] Petrov D S, Gangardt D M and Shlyapnikov 2004 *Journal de Physique IV Proceedings* **116** 5
[25] Colcelli A, Defenu A, Mussardo G and Trombettoni A 2020 *Phys. Rev. B* **102** 184510
[26] Smerzi A, Fantoni S, Giovanazzi S and Shenoy S R 1997 *Phys. Rev. Lett.* **79** 4950
[27] Jaksch D, Bruder C, Cirac J I, Gardiner C W and Zoller P 1998 *Phys. Rev. Lett.* **81** 3108
[28] Trombettoni A and Smerzi A 2001 *Phys. Rev. Lett.* **86** 2353
[29] Masi L, Petrucciani T, Ferioli G, Semeghini G, Modugno G, Inguscio M and Fattori M 2021 *Phys. Rev. Lett.* **127** 020601
[30] Javanainen J and Yoo S M 1996 *Phys. Rev. Lett.* **76** 161
[31] Smerzi A and Raghavan S 2000 *Phys. Rev. A* **61** 063601
[32] Dalton B and Ghanbari S 2012 *J. Mod. Opt.* **59** 287
[33] Grond J, Hohenester U, Mazets I and Schmiedmayer J 2010 *New J. Phys.* **12** 065036
[34] Wineland D, Bollinger J, Itano W and Heinzen D 1994 *Phys. Rev. A* **50** 67
[35] Deutsch C, Ramirez-Martinez F, Lacroûte C, Reinhard F, Schneider T, Fuchs J N, Piéchon F, Laloë F, Reichel J and Rosenbusch P 2010 *Phys. Rev. Lett.* **105** 020401
[36] Lücke B *et al* 2011 *Science* **334** 6057
[37] Gerry C C and Mimih J 2010 *Contemp. Phys.* **51** 497
[38] Goussev A, Jalabert R A, Pastawski H M and Wisniacki D A 2012 *Scholarpedia* **7** 11687